Liquid Crystals

Publication details, including instructions for authors and subscription information:
http://www.informaworld.com/smpp/title~content=t713926090

A thin cell dielectric spectroscopy method for liquid crystals

Bo Gestblom[a]; Stanislaw Wróbel[b]
[a] Department of Physics, Uppsala University, Uppsala, Sweden [b] Institute of Physics, Jagellonian University, Kraków, Poland

To cite this Article Gestblom, Bo and Wróbel, Stanislaw(1995) 'A thin cell dielectric spectroscopy method for liquid crystals', Liquid Crystals, 18: 1, 31 — 35

To link to this Article: DOI: 10.1080/02678299508036587

URL: http://dx.doi.org/10.1080/02678299508036587

LIQUID CRYSTALS, 1995, VOL. 18, NO. 1, 31–35

A thin cell dielectric spectroscopy method for liquid crystals

by BO GESTBLOM*
Department of Physics, Uppsala University, Box 530, S-75121 UPPSALA, Sweden

and STANISLAW WRÓBEL
Institute of Physics, Jagellonian University, 30059 Kraków, Poland

(*Received 18 February 1994; accepted 6 May 1994*)

A thin cell method for dielectric time domain spectroscopy is described. The cell allows one to study the dielectric dispersion and absorption spectra for both components of the dielectric permittivity tensor of uniaxial systems like nematic and smectic A and B phases. Results are presented for 4-*n*-pentyl-4′-cyanobiphenyl in the isotropic phase and upon orientation in the nematic phase.

1. Introduction

In dielectric time domain spectroscopy (TDS) the permittivity spectrum of a dielectric is determined from its influence on the shape of a pulse propagating in a transmission line. By Fourier transformation of pulse shapes the dielectric spectrum can—from a single measurement—be determined over a wide frequency range. Various arrangements of the dielectric sample in the line have been considered [1]. In the first TDS measurements, the dielectric filled a long section of the transmission line and the first reflection of an incoming pulse against the air–sample interface was studied. This method may give the spectrum to high frequencies, but suffers from the drawback of requiring a large sample volume [2]. By reducing the sample length, either the totally transmitted or totally reflected pulse shape may be studied. In transmission studies sample lengths of the order of cm have been used [3, 4]. Smaller sample volumes can give sufficient information in the reflected line shape if the sample ends the open circuited line [5, 6]. Cell lengths of the order of mm–cm are in this case typical. However, by using a flat ended coaxial line pressed against or immersed into the dielectric, frequencies up to the order 10 GHz can be used where the sample depth is less than 1 mm [7, 8].

In both the reflection and transmission methods, the measuring cells are readily made from standard coaxial components. For liquids, the dielectric sample is easily inserted and removed from the cell. For the reflection method, sample volumes of the order of 0·1 ml can be sufficient. Together with the wide frequency coverage from the MHz region up to the order 10 GHz, this makes the TDS method attractive for studies of molecular motion, in for instance liquid crystals. In the case of ferroelectric liquid crystals (FLC) and some new materials for science and technology, it is important to obtain all physical characteristics on very small samples. In such studies, it is valuable also to be able to study the dielectric properties in the presence of orienting external electric or magnetic fields in order to study tensorial properties. An orienting magnetic field can be applied along the coaxial line, i.e. perpendicular to the measuring electric field. However, the coaxial geometry does not allow direct application of an external orienting magnetic field parallel to the measuring electric field. The wide gap between the coaxial electrodes in the line also makes it difficult to apply a strong electric field.

These drawbacks can be circumvented by arranging the cell in the form of a lumped capacitance at the end of the coaxial line [9]. By making the capacitor thin, the sample volume can be reduced, and amounts of substance of the order μl may be sufficient. The thin cell also makes it possible to apply a strong orienting electric field, with a voltage sufficiently low not to ruin the sampling heads of the oscilloscope, used to register the line shapes studied. The end capacitor also allows the application of an orienting external magnetic field both perpendicular and in parallel to the measuring electric field. In this paper a thin cell end capacitance method is described, and its potential in studying liquid crystals in the presence of orienting fields is demonstrated by measuring the permittivity spectrum of 4-*n*-pentyl-4′-cyanobiphenyl (5CB), which exhibits the following phase sequence [10]:

C 22·5°C N 35·2°C I.

The sample used was synthesized by Merck Ltd, UK.

---

*Author for correspondence.

2. Theory

In a TDS reflection measurement, an incident step pulse $v(t)$ propagating in a coaxial line will, on reaching a dielectric sample, introduce a reflected pulse $r(t)$. The pulse shapes are recorded by a sampling oscilloscope, and the signal is converted into the frequency domain by Fourier transformation

$$\left.\begin{aligned} R(\omega) &= \int_0^\infty r(t)\exp(-i\omega t)\,dt, \\ V(\omega) &= \int_0^\infty v(t)\exp(-i\omega t)\,dt. \end{aligned}\right\} \tag{1}$$

The incident and reflected voltages will be related to the input admittance of the considered line section by the current/voltage ratio

$$Y = G\cdot\frac{(V-R)}{(V+R)}, \tag{2}$$

where G is the characteristic admittance of the line.

In a real measurement, the incident line shape $v(t)$ is not readily determined with sufficient accuracy, and it is better to compare the reflected line shape from the unknown dielectric, $v_x(t)$, with that reflected from a reference of known dielectric properties $v_r(t)$. As shown by Cole [11], the difference in admittance between the two cases is given by

$$\frac{Y_x}{G} - \frac{Y_r}{G} = \frac{\left(1 - \left(\dfrac{Y_r}{G}\right)^2\right)\dfrac{R_r - R_x}{R_r + R_x}}{1 + \dfrac{Y_r}{G}\cdot\dfrac{R_r - R_x}{R_r + R_x}}. \tag{3}$$

Here R_x and R_r are the transforms of the reflected line shapes from the unknown and the reference dielectric, respectively. The admittance difference is a bilinear form in $(R_r - R_x)/(R_r + R_x)$.

If the admittance considered consists of a dielectric filled end capacitance C_0, then $Y_x = i\omega C_0\varepsilon_x^*$. Here $\varepsilon_x^* = \varepsilon_x' - i\varepsilon_x''$ is the complex permittivity of the unknown dielectric. With air as reference, i.e. the reflection from an empty cell constitutes the reference R_1, we obtain

$$\varepsilon_x^* - 1 = \frac{\dfrac{G}{i\omega C_0}\left(1 - \left(\dfrac{i\omega C_0}{G}\right)^2\right)\dfrac{R_1 - R_x}{R_1 + R_x}}{1 + \dfrac{i\omega C_0}{G}\cdot\dfrac{R_1 - R_x}{R_1 + R_x}}. \tag{4}$$

Putting $C_0/G = k$, the permittivity of the unknown dielectric can now be obtained from

$$\varepsilon_x^* - 1 = \frac{(1 + k^2\omega^2)\dfrac{\rho}{ik\omega}}{1 + ik\omega\rho}, \tag{5}$$

where

$$\rho = \frac{R_1 - R_x}{R_1 + R_x}. \tag{6}$$

If the end capacitance consists of an open-ended section of the coaxial line with outer and inner radii r_y and r_i, respectively and of length d, the specific admittance $G = 2\pi\sqrt{(\varepsilon_0/\mu_0)}/\ln r_y/r_i$, while the capacitance $C_0 = 2\pi\varepsilon_0 d/\ln r_y/r_i$. This gives the cell constant $k = d/c$, where c is the speed of light in free space. k is then in principle known from the cell length.

For other shapes of the end capacitance, the value of the cell constant k may not be so easily calculated. However, for an ideal capacitance ending an ideal coaxial line, the cell constant k can be determined from a standard dielectric of known permittivity.

As discussed by Cole [11], deviations from an ideal coaxial line-end capacitance system, will introduce extraneous reflections making equation (5) not strictly valid. However, the admittance measured at one point in the coaxial is a bilinear form of the admittance at another point. As pointed out by Cole, this implies that the bilinear form in the working relation for ε^* can be retained.

$$\varepsilon_x^* = \frac{1 + A\rho}{1 - B\rho}. \tag{7}$$

The $A = A' + iA''$ and $B = B' + iB''$ coefficients will now differ from the simple values suggested by equation (4), but will correct for imperfections in the line and connectors. To calibrate the cell and determine the A and B coefficients, two standard dielectrics have to be used.

3. Experimental

The construction of a thin end capacitance cell is shown in figure 1. At the end of a standard 7 mm inner diameter coaxial air line, a Kel-F disc holds the centre conductor of 3 mm diameter, which constitutes one electrode of the end capacitance. An end cap, which can be tightened to the line, constitutes the other electrode. A thin mylar ring of suitable thickness acts as spacer between the electrodes. Two small holes are drilled through the end cap to allow the insertion and removal by a syringe of the liquids studied. Cleaning and drying of the cell between change of liquids is easily done by flushing a suitable solvent through the cell without need for its disassembly. The temperature is controlled by surrounding the line with a thermostatted jacket.

The step pulse used was obtained from an HP 1106B pulse generator, and the reflected pulse shapes were monitored by an Iwatsu SAS 8310 Wave Form Analyser. The analyser was controlled by a PC which also performed the Fourier transformations. Two time windows were used in measuring the reflected line shapes—10 ns and 100 ns. The A and B coefficients were determined by solving equation (6) for standard dielectrics, heptane/acetone for the high frequency end of the spectrum and chloroform/

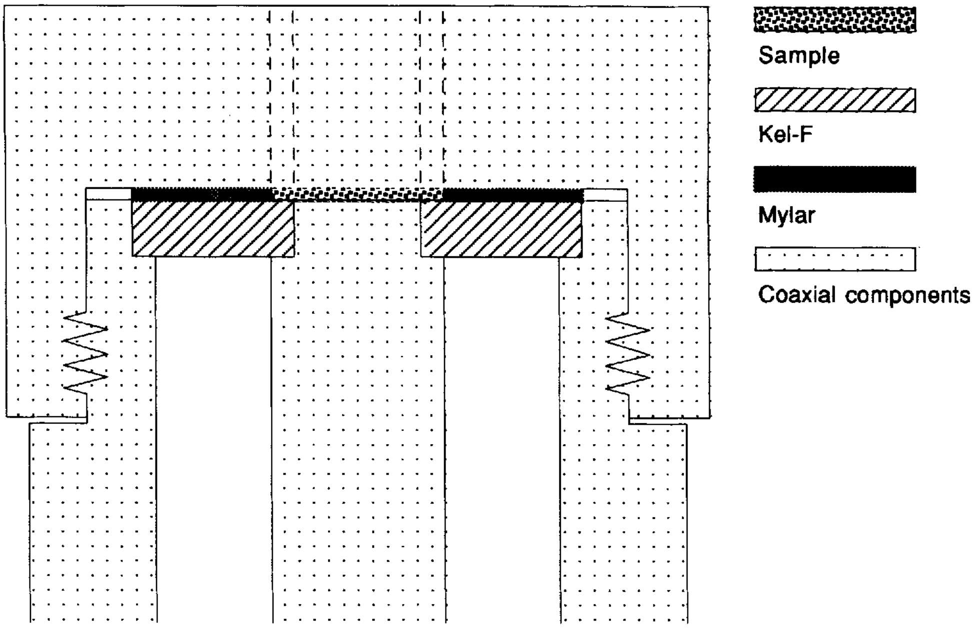

Figure 1. The thin sample cell design showing 7 mm live to APC7–SMA adapter.

acetone below the GHz range. With a 50 μm mylar spacer, the cell constant k corresponds to a coaxial cell length of 1 cm, i.e. the same response is obtained from a minute fraction of substance with the thin cell as from a long coaxial cell filled with the dielectric.

The orienting magnetic field was supplied by an electromagnet, whereby the planar alignment can be easily obtained by putting the end of the coaxial line between the magnetic poles. For homeotropic alignment, a coil with an iron core placed against the end cap of the cell gives a sufficiently uniform field inside the cell. An orienting electric field could be applied by inserting a bias tee and DC block Picosecond Pulse Labs 5530A in the coaxial line. This allows the application of up to 200 V over the capacitor, while the block passes the fast-rising measuring step pulse with little degradation.

4. Results

The permittivity spectrum of 4-*n*-pentyl-4′-cyanobiphenyl in the isotropic phase at 40°C is shown in figure 2. The spectrum is slightly broader than which corresponds to a single relaxation time and was fitted using a least squares fit procedure to the Cole–Cole model function

$$\varepsilon^* = \varepsilon_\infty + \frac{\varepsilon_s - \varepsilon_\infty}{1 + (i\omega\tau)^{1-\alpha}}. \tag{8}$$

The theoretical spectrum calculated with the parameters $\varepsilon_s = 10{\cdot}9$, $\varepsilon_\infty = 2{\cdot}8$, $\tau = 4{\cdot}1$ ns and $\alpha = 0{\cdot}12$ is shown by the full line.

The sample was then slowly cooled to 30°C into the nematic phase with a magnetic field of about 0·6 T applied parallel to the electrodes. The permittivity spectrum is shown in figure 3 (crosses). The sample was reheated to 40°C and again slowly cooled down to 30°C, this time with an electric field perpendicular to the electrodes, obtained by applying a voltage of 30 V across the cell. The resulting permittivity spectrum is included in figure 3 (circles). The full dispersion could not be covered for the latter case within the accessible frequency range. However, a sufficiently large part of the spectrum is covered to allow a fit to the Cole–Cole function equation (7). The theoretically calculated spectra included in figure 3 have been calculated with the parameters $\varepsilon_s = 7{\cdot}7$, $\varepsilon_\infty = 2{\cdot}4$, $\tau = 3{\cdot}5$ ns and $\alpha = 0{\cdot}30$ (full line) and $\varepsilon_s = 21{\cdot}1$, $\varepsilon_\infty = 3{\cdot}1$, $\tau = 30$ ns and $\alpha = 0{\cdot}06$ (broken line), respectively. The spectra obtained by the TDS thin cell method agree quite well with those measured by frequency domain methods [10, 12].

The experimental data fit rather well to a symmetric Cole–Cole distribution. A better fit is not obtained with the Cole–Davidson equation, also used to describe the dielectric spectra of *n*CBs [13, 14]. Perhaps the latter model is better for *n*CBs with longer alkyl chains. It is worth noting that for 7CB [15], a pure Debye type spectrum was observed over a wide temperature range of the isotropic phase. The dielectric spectrum observed for the perpendicular component is broad and one can fit two (or more) Debye functions, as has been done before for 8CB [16].

5. Discussion

Most liquid crystalline phases exhibit anisotropic properties [17], i.e. their physical quantities such as

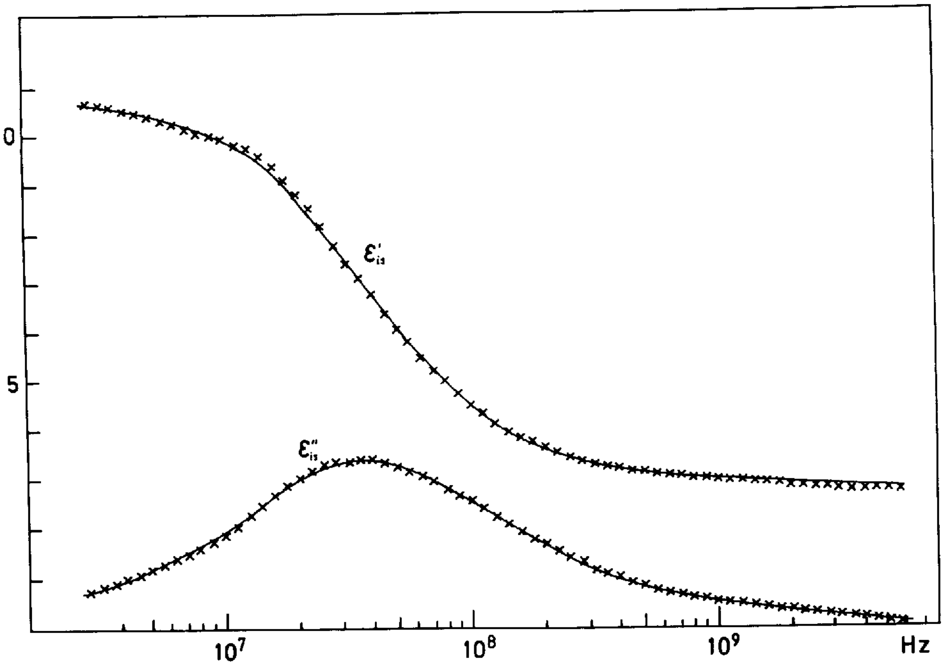

Figure 2. The dielectric permittivity spectrum of 5CB at 40°C (isotropic phase).

dielectric permittivity, magnetic susceptibility, diffusion coefficient, viscosity and so on are second order tensors. To study such materials, one should measure all components of the tensor quantities. For instance, in the case of uniaxial liquid crystals (nematic, smectic A and B), the dielectric permittivity tensor in the laboratory frame $(x; y; z)$ has the following form:

$$\varepsilon_{ij} = \begin{pmatrix} \varepsilon_\perp & 0 & 0 \\ 0 & \varepsilon_\perp & 0 \\ 0 & 0 & \varepsilon_\parallel \end{pmatrix}, \qquad (9)$$

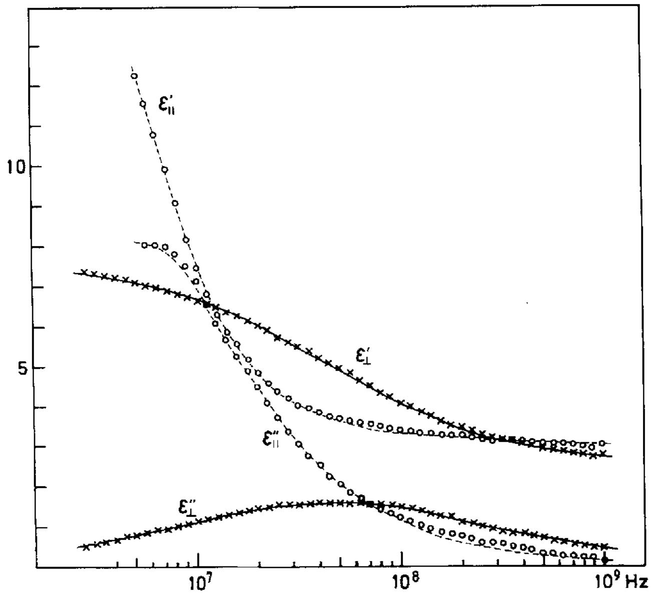

Figure 3. The dielectric spectra of 5CB at 30°C obtained for both principal directions of the oriented nematic phase; crosses: magnetic field parallel to electrodes; circles: electric field perpendicular to electrodes. Calculated spectra are indicated by the full and dashed line (see text for detail).

where the optical axis of the liquid crystal is parallel to the z-axis, coinciding usually with the external aligning magnetic or electric field. The difference between the two principal components measured parallel ($\varepsilon_\parallel$) and perpendicular ($\varepsilon_\perp$) to the aligning field is called the dielectric anisotropy. Depending on molecular structure and phase structure, the dielectric anisotropy can be positive or negative.

Good examples of substances having a positive dielectric anisotropy are the 4-alkyl-4′-cyanobiphenyls (*n*CBs) [10] $H_{2n+1}C_n$–C_6H_4–C_6H_4–CN.

Their nematic phases align easily in external electric fields in such a way that the long axis of the molecules are on average parallel to the aligning electric field. In this case, one obtains the so-called homeotropic texture in which the molecular long axes are on average perpendicular to the electrodes. Having a homeotropic texture, one can measure the $\varepsilon_\parallel$ component of the dielectric permittivity. The homeotropic alignment can also be obtained by applying a strong magnetic field ($B > 0{\cdot}5$ T) perpendicular to the electrodes. To obtain the so-called planar texture one should in the case of *n*CBs apply a strong magnetic field parallel to the surface of the electrodes. In this geometry, the $\varepsilon_\perp$ component can be measured.

The transition temperature form the isotropic to the nematic phase of 5CB is 35·2°C. The strong positive dielectric anisotropy of 5CB in the nematic phase at 30°C is illustrated in figure 3. The long relaxation time observed for the $\varepsilon_\parallel$ spectrum is connected to the reorientation of elongated molecules around their short axes. The dielectric spectrum acquired for the perpendicular component is complex and may be influenced by at least two molecular mechanisms, namely the reorientation around the long axis and the stochastic precession.

The permittivity spectra show a good fit to the Cole–Cole model function as seen in figure 3. No indication of secondary dispersions at frequencies above the dominant dispersion, as reported for 7CB and 8CB [18], can be found for this shorter homologue, 5CB.

Finally, one should point out that up to now there have been a few papers reporting high frequency dielectric studies on thin layers made by using frequency domain techniques, which allow dielectric measurements up to 1 GHz [19–21]. However, in some cases, only one component of the dielectric permittivity tensor could be measured.

6. Conclusions

The method described allows one to measure both components of the dielectric permittivity tensor of uniaxial systems. For nematics exhibiting a strong positive dielectric anisotropy, one can obtain the homeotropic alignment by means of a DC electric field. The homeotropic or planar textures can also be obtained by application of a magnetic field, and it is easy to switch from one alignment to the other.

As for coaxial cells used earlier, this TDS method allows the measurement of the permittivity spectrum over a large frequency range, also reaching in to the GHz region. The fast molecular motions connected with the reorientation around the molecular long axis can then be studied. In addition to the orientation possibilities, the present cell has the advantage that only a very small amount of substance is needed, and this is important for the study of liquid crystals.

References

[1] For reviews see: VAN GEMERT, M. J. C., 1973, *Philips Res. Rep.*, **28,** 530. COLE, R. H., 1977, *A. Rev. phys. Chem.*, **28,** 283. FELDMAN, Y. D., ZUEV, Y. F., POLYGALOV, E. A., and FEDOTOV, V. D., 1992, *Coll. Polym. Sci.*, **270,** 768.

[2] GESTBLOM, B., and NORELAND, E., 1984, *J. phys. Chem.*, **88,** 664.

[3] GESTBLOM, B., and NORELAND, E., 1977, *J. phys. Chem.*, **81,** 782.

[4] GESTBLOM, B., and ELMGREN, H., 1982, *Chem. Phys. Lett.*, **90,** 412.

[5] COLE, R. H., 1975, *J. phys. Chem.*, **79,** 1469.

[6] COLE, R. H., MASHIMO, S., and WINSOR, P., 1980, *J. phys. Chem.*, **84,** 786.

[7] GABRIEL, C., GRANT, E. H., and YOUNG, I. R., 1986, *J. Phys.* E, **19,** 843.

[8] SHINYASHIKIKI, N., ASAKA, N., MASHIMO, S., YAGIHARA, S., and SASAKI, N., 1990, *Biopolymers*, **29,** 1185.

[9] IKSANDER, M. F., and STUCHLY, S. S., 1972, *I.E.E.E. Trans. Instrum. Meas.*, **21,** 425.

[10] LIPPENS, D., 1978, Thesis, L'Université de Lille.

[11] COLE, R. H., BERBERIAN, J. G., MASHIMO, S., CHRYSSIKOS, G., BURNS, A., and TOMBARI, E., 1989, *J. appl. Phys.*, **66,** 793.

[12] KREUL, H. G., URBAN, S., and WÜRFLINGER, A., 1992, *Phys. Rev.* A, **45,** 3624.

[13] PARNEIX, J. P., LEGRAND, C., and DECOSTER, D., 1983, *Molec. Crystals liq. Crystals*, **98,** 361.

[14] BUKA, A., and PRICE, A. H., 1985, *Molec. Crystals liq. Crystals*, **116,** 187.

[15] DAVIES, M., MOUTRAN, R., PRICE, A. G., BEEUERS, M. S., and WILLIAMS, G., 1976, *J. chem. Soc. Faraday Trans. II*, **72,** 1447.

[16] DRUON, C., and WACRENIER, J. M., 1978, *Ann. Phys.*, **3,** 199.

[17] DE GENNES, P. G., 1974, *The Physics of Liquid Crystals* (Clarendon Press).

[18] BOSE, T. K., CAMPBELL, B., YAGIHARA, S., and THOEN, J., 1987, *Phys. Rev.* A, **36,** 5767.

[19] PFEIFFER, M., HILLER, S., WRÓBEL, S., and HAASE, W., 1993, *Ferroelectrics*, **147,** 419.

[20] KREMER, F., VALLERIEN, S. U., and SCHOENFELD, A., 1991, *Ferroelectrics*, **121,** 69.

[21] JADZYN, J., LEGRAND, C., ZYWUCHI, B., CZECHOWDKI, G., and DABROWSKI, R., 1992, *SPIE. Liquid Crystals and Solid Crystals* , Vol. 1845, 497.